

Comment on 'Initiation of chromosome replication controls both division and replication cycles in *E. coli* through a double-adder mechanism'

Guillaume Le Treut^{1*}, Fangwei Si^{1*}, Dongyang Li^{1*}, and Suckjoon Jun^{1,2**}

¹ Department of Physics, University of California, San Diego, La Jolla, CA 92093, USA

² Section of Molecular Biology, Division of Biology, University of California, San Diego, La Jolla, CA 92093, USA

* These authors contributed equally to this work

** Correspondence: suckjoon.jun@gmail.com

Abstract

Witz *et al.* recently performed single-cell mother machine experiments to track growth and the replication cycle in *E. coli*. They analyzed the correlation structure of selected parameters using both their data and published data, and concluded that *E. coli* cell-size control is implemented at replication initiation, which challenged the newly emerged division-centric mechanism of cell-size control in bacteria. We repeated Witz *et al.*'s analysis, and performed additional experiments and analytical calculations. These results explain Witz *et al.*'s observation and in fact support the division-centric model.

Introduction

Cell size control is one of the long-standing problems in biology (Jun *et al.* 2018). The recent discovery of the adder principle has demonstrated that many evolutionary divergent organisms in both bacteria and eukaryotes share the same homeostasis strategy for size control despite their differences in molecular details and biological complexity (Campos *et al.* 2014; Taheri-Araghi *et al.* 2015; Jun and Taheri-Araghi 2015). This makes bacteria an attractive and tractable system to understand the mechanistic origin of cell-size control.

An outstanding issue in bacterial cell-size control is about what physiological parameters size control is imposed on. For example, the celebrated Helmstetter-Cooper model established three physiological parameters are necessary and sufficient to completely describe the progression of bacterial cell cycle and cell size (Cooper and Helmstetter 1968). Helmstetter and Cooper chose the growth rate (λ), cell size at replication initiation (S_i), and the time elapsed during DNA replication and the subsequent cell division (C+D) (Figure 1A). Therefore, their model is often interpreted as replication initiation being a major implementation point of cell-cycle control. Formally, however, other sets of three independent parameters (Figure 1A) could constitute a cell-size control model.

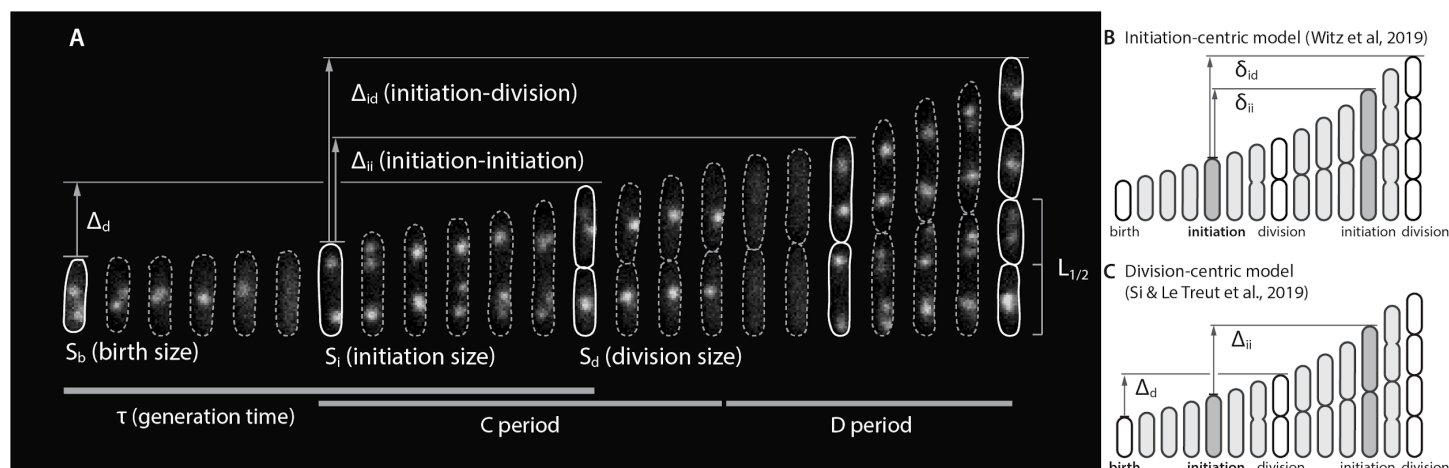


Figure 1: Physiological parameters that can be measured from single-cell experiments. **A.** The Helmstetter-Cooper model describes cell size and cell cycle using three parameters: generation time τ , C+D, and the initiation size S_i . Additional parameters that can be measured include size added between two consecutive initiations $\Delta_{ii} = \delta_{ii} \times N_{ori}$, size added between two consecutive divisions Δ_d , size added between initiation and division $\Delta_{id} = \delta_{id} \times N_{ori}$, relative septum position $L_{1/2}$, and the elongation rate $\lambda = d\ln(l)/dt$, where l is the cell length (not shown). **B.** The initiation-centric model by Witz et al. (2019) proposed λ , δ_{ii} , and δ_{id} (lower-cases δ 's indicate size normalized per origin) as the independently physiological parameters, whereas **C.** the division-centric model by Si & Le Treut et al. (2019) has proposed λ , δ_{ii} , and Δ_d as independent physiological parameters. Note that δ_{id} can span multiple generations, as the C+D period can in the Helmstetter-Cooper model. The number of origins in Witz et al.'s initiation-centric model is therefore determined by δ_{id}/δ_{ii} , similar to $(C+D)/\tau$ in the Helmstetter-Cooper model. By contrast, in the division-centric model by Si and Le Treut et al., the added sizes Δ_d and Δ_{ii} are between two consecutive cell cycles.

The recent eLife paper by Witz et al. (Witz, van Nimwegen, and Julou 2019) revisited the question of implementation point for cell size control. To this end, they tracked replication and division cycles at the single-cell level, using methods similar to previous works (Wallden et al. 2016; Si and Le Treut et al. 2019; Adiciptaningrum et al. 2015). They computed correlations between all pairs of measured physiological parameters, and identified a set of most mutually uncorrelated parameters. They then assumed that statistically uncorrelated physiological parameters must represent biologically independent controls. Such approaches previously facilitated the discovery of the adder principle and its formal description (Taheri-Araghi et al. 2015). Based on the correlation analysis, Witz et al. concluded that cell size at replication initiation is the most likely implementation point of size control, supporting previous theoretical models of initiation-centric size control (Amir 2014, 2017) but directly contradicting the division-centric mechanism revealed in our previous work (Si and Le Treut et al. 2019).

Here, we repeated Witz et al.'s analysis and also performed additional experiments and modeling as detailed below. We show that (1) Witz et al.'s own analysis of published data in fact supports the division-centric model. (2) Our new experiments using the *E. coli* BW strain that has the genetic background similar to Witz *et al.*'s also support the division-centric model. (3) In general, their correlation-based approach cannot distinguish different models. (4) Their initiation-centric double-adder model is analytically inconsistent with the adder phenotype and, in fact, produces a sizer-like behavior, making it an unlikely model of cell-size homeostasis in bacteria.

We expect the experiment, analysis, and modeling presented in this work to be a useful resource for researchers who are considering interdisciplinary, single-cell approaches to quantitative microbial physiology.

Results

Summary of Witz *et al.*'s correlation approach and results.

We first summarize the results of correlation analysis in Witz et al. (2019). They considered a total of 10 measured parameters and 10 derived parameters, some of which are shown in Figure 1A. Since the work by Helmstetter and Cooper (1968), it has been known that the progression of cell size and cell cycle can be completely described using 3 variables (Wallden et al. 2016; Si et al. 2017). Therefore, there are at most $C_{20}^3 = 1140$ possible combinations. To measure the statistical independence of each set of parameters, Witz et al. constructed a correlation matrix (Figure 2).

$$\begin{pmatrix} 1 & C_{ab} & C_{ac} \\ C_{ba} & 1 & C_{bc} \\ C_{ca} & C_{cb} & 1 \end{pmatrix}$$

Figure 2: Correlation matrix.

The diagonal elements are 1's and the off-diagonal elements are cross-correlations between pairs of parameters (a, b and c). Therefore, if all parameters are statistically independent of each other, the off-diagonal elements should be 0, and the determinant I of the matrix should be 1 (Figure 2). Based on this observation, Witz *et al.* used the determinant $I \leq 1$ of the matrix as a metric for statistical independence of the hypothetical control parameters, with $I = 1$ being the set of most independent parameters. Note that Witz *et al.* analyzed a set of 4 parameters, instead of 3, out of the 20 aforementioned parameters to compute I (see next section and Materials and Methods).

To generate single-cell data, Witz *et al.* performed four mother machine experiments for three different growth conditions (Witz, van Nimwegen, and Julou 2019). In addition, they also chose to analyze one of the 9 nutrient-limitation experiment data sets from Si & Le Treut *et al.* (2019). They found the following four parameters to be statistically most independent and produce the highest value of I : λ (elongation rate), δ_{ii} (size added from initiation to initiation per origin), δ_{id} (size added from initiation to division per origin), and Λ_i (initiation mass per origin).

They concluded that replication initiation is the most upstream control of cell size (via δ_{ii} and Λ_i), as division is triggered after growing by a constant size per origin since initiation (δ_{id}) via an unknown mechanism (Figure 1B). This last point is initiation-centric and directly contradicts our previous findings that (1) replication and division are independently controlled via three parameters λ , δ_{ii} and Δ_d at the mechanistic level in both *Escherichia coli* and *Bacillus subtilis*; (2) it is cell division, not replication initiation, that drives cell-size homeostasis (Si and Le Treut *et al.* 2019).

The result of Witz *et al.*'s correlation approach is more consistent with the division-centric model, rather than the initiation-centric model.

Since the initiation-centric model and division-centric model are mutually exclusive (see next section for correlation analysis), we were initially puzzled that the experiment in Si & Le Treut *et al.* (2019) supported the initiation-centric model. However, this particular experiment was a special case, because that was the slow growth condition wherein *E. coli* deviated from the adder phenotype (Wallden *et al.* 2016; Si and Le Treut *et al.* 2019). This deviation is caused by active degradation of FtsZ by ClpXP in slow growth conditions (Männik, Walker, and Männik 2018; Sekar *et al.* 2018; Si and Le Treut *et al.* 2019), which we mechanistically explained by demonstrating that repression of clpX restores the adder phenotype (Si and Le Treut *et al.* 2019).

We therefore set out to re-analyze all our 9 steady-state nutrient-limitation growth experiments in *E. coli* and *B. subtilis* using the same approach Witz *et al.* used. We analyzed a set of 3 parameters as defined in Figure 1B and 1C, instead of 4 parameters. This difference in the number of parameters does not affect the overall conclusion of the I -value analysis (see Materials and Methods). We computed I values for three models: the “initiation-

centric” adder model (Witz, van Nimwegen, and Julou 2019), the “division-centric” adder model (Si and Le Treut et al. 2019), and also the classic Helmstetter-Cooper model (Cooper and Helmstetter 1968) as a reference.

The results of the analysis are clear (Figure 3). Out of the total of nine experiments that we analyzed using Witz *et al.*'s method, six experiments were more consistent with the division-centric model (Si and Le Treut et al. 2019). On the other hand, both models performed consistently better than the Helmstetter-Cooper model.

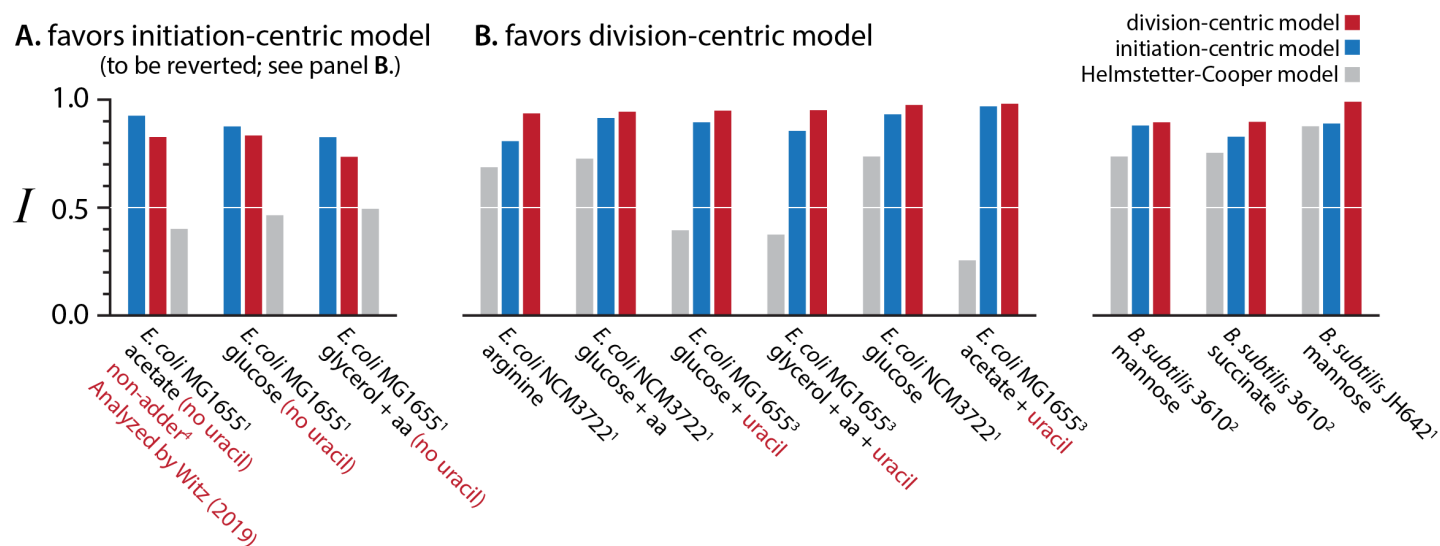


Figure 3: Data in *E. coli* and *B. subtilis* support the division-centric model (Si & Le Treut et al., 2019), rather than the initiation-centric model (Witz et al., 2019) or the Helmstetter-Cooper model (1968). (A). Our MG1655 data initially supported the initiation-centric model. However, this was due to the well-known pyrimidine pseudo-auxotrophy in MG1655 (Soupene et al. 2003). To alleviate the growth defect, we supplemented growth media with uracil, and the results reverted (B). All other published data supported the division-centric model. Superscripts represent the data sources: 1 - Si & Le Treut et al., 2019, 2 - Sauls et al., 2019, 3 - Jun lab unpublished results. See Materials and Methods for our analysis methods.

The correlation structure in the MG1655 strain in Si & Le Treut *et al.* (2019) is due to pyrimidine pseudo-auxotrophy.

While six out of nine experiments were in favor of the division-centric model, there were still three experiments that were more consistent with the initiation-centric model (which includes the aforementioned experiment in which the adder phenotype breaks; Figure 3). However, we noticed that the three experiments used the same strain with the genetic background of *E. coli* K-12 MG1655. Kustu and colleagues extensively studied the growth physiology of MG1655 (Soupene et al. 2003). Among the several growth defects, *rph-1* is known to cause pyrimidine pseudo-auxotrophy in MG1655. While pyrimidine pseudo-auxotrophy *per se* does not affect the adder phenotype as shown before (Si and Le Treut et al. 2019; Campos et al. 2014), it could affect correlation structures involving other physiological parameters. Fortunately, in MG1655, pyrimidine pseudo-auxotrophy can be alleviated by supplementing the growth media with uracil (Soupene et al. 2003). Indeed, the three experiments supporting the initiation-centric model lacked the uracil supplement.

Following the study by Kustu and colleagues, we repeated our experiments using uracil supplemented media. This reverted the correlation structure of the three experiments, and the MG1655 also supported the division-centric model (Figure 3). These results suggest that pyrimidine pseudo-auxotrophy affects the correlation structure observed in MG1655 in Si & Le Treut et al. (2019). With the physiological defect fixed, all our experiments in both *E. coli* and *B. subtilis* unanimously supported the division-centric model.

The *E. coli* BW strains also support the division-centric model.

We next asked why Witz *et al.*'s own data supported their initiation-centric model, and repeated the *I*-value analysis of all their pre-processed four datasets (Materials and Methods). To our surprise, our own analysis showed that their data are in fact more consistent with the division-centric mode (Figure 4A).

To ensure our results are correct, we also repeated experiments using an *E. coli* K-12 strain with a genetic background practically identical to the one used in Witz *et al.* Two notable differences in experimental methods between our two studies are the choice of strains and how replication cycles were tracked at the single-cell level. For example, Witz *et al.* used *E. coli* BW27378. This is one of the widely adopted strains because it was used by Barry Wanner (BW) for the development of the λ red system (Datsenko and Wanner 2000) and subsequently the Keio collection (Baba *et al.* 2006). Incidentally, BW27378 also has the *rph-1* mutation, although it is not known whether the strain also exhibits pyrimidine pseudo-auxotrophy as in MG1655.

To track replication cycles, Witz *et al.* used FROS (fluorescent repressor-operator system) with a well-known LacI-mVenus and the LacO cassette inserted near *oriC*. This method in principle allows detection of replication initiation by measuring the timing the duplicated origin splits. There are two main caveats with this approach: (1) the measured initiation timing is almost always delayed by an uncontrolled amount of time because of the extensively studied phenomena of origin cohesion (Lesterlin *et al.* 2012; Sunako, Onogi, and Hiraga 2001), i.e., duplicated origins stay together for different durations of time under different growth conditions (2) this method cannot detect termination of replication. By contrast, the replisome-based tracking of DNA replication does not suffer from these caveats.

We thus transduced *dnaN-YPet* (encodes for the β sliding clamp in the replisome) to BW25113 (almost identical genetic background as Witz *et al.*'s BW27378) and repeated the experiments (Materials and Methods). Consistent with our analysis results of Witz *et al.*'s data, we found that data from these new experiments also supported the division-centric model (Figure 4B), with or without uracil supplement. While it is beyond the scope of this work to study details of physiological properties specific to the BW strains, it is clear that all experimental results support the division-centric model.

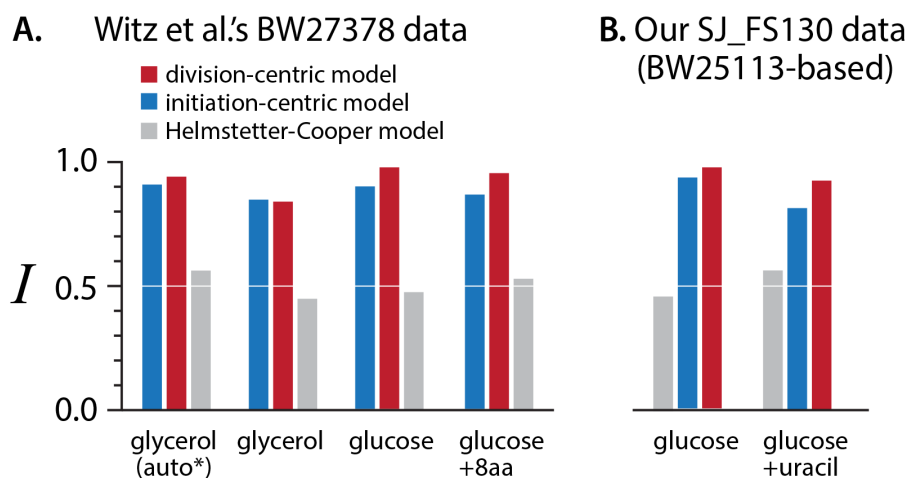


Figure 4: Results of the BW strains used in Witz *et al.* (A) and our new experiment (B). The glycerol (auto*) is the same experiment as glycerol, but Witz *et al.* used automated image analysis for detecting replication initiation.

In the following two sections, we switch our focus from experiment to modeling, and show that the initiation-centric model based on the four parameters derived in Witz *et al.* (2019) cannot reproduce size homeostasis by the adder principle.

The *I*-value analysis is insensitive to differences between size-control models

While our analysis shows that the single-cell data is more consistent with the division-centric model than the initiation-centric model, the *I* values of both models were close to 1 and their differences were typically less than 10%. This raises the question whether the *I*-value analysis can really identify the correct size control model based on the *I* values. Therefore, we have computed the *I* values for all combinations of 3 among 18 variables (total of 816) using the experimental dataset analyzed by Witz and colleagues (their figure 7). The division-centric and the replication-centric models had high scores, ranking 57th and 88th respectively, yet other combinations of variables had even higher *I* values. In addition to the one condition analyzed by Witz *et al.*, we also performed the analysis on the other 3 conditions of their study. Overall, we found that the division-centric model always had a higher *I* value than the replication centric model with only one exception of glycerol condition (Figure 4A). We also repeated the analysis using experimental data from the 6 conditions published in Si & Le Treut (2019), and obtained similar results.

Most importantly, the rank-ordered *I* values showed smooth changes from the highest value to the lowest value from the data in both studies. For this type of dimensional reduction approach to be useful (such as the principal component analysis), the *I* values ideally should show an abrupt transition such that only a small fraction of the models have significantly higher *I* values than the rest. Based on our results, we conclude that the *I*-value analysis cannot reveal true (independent) control parameters.

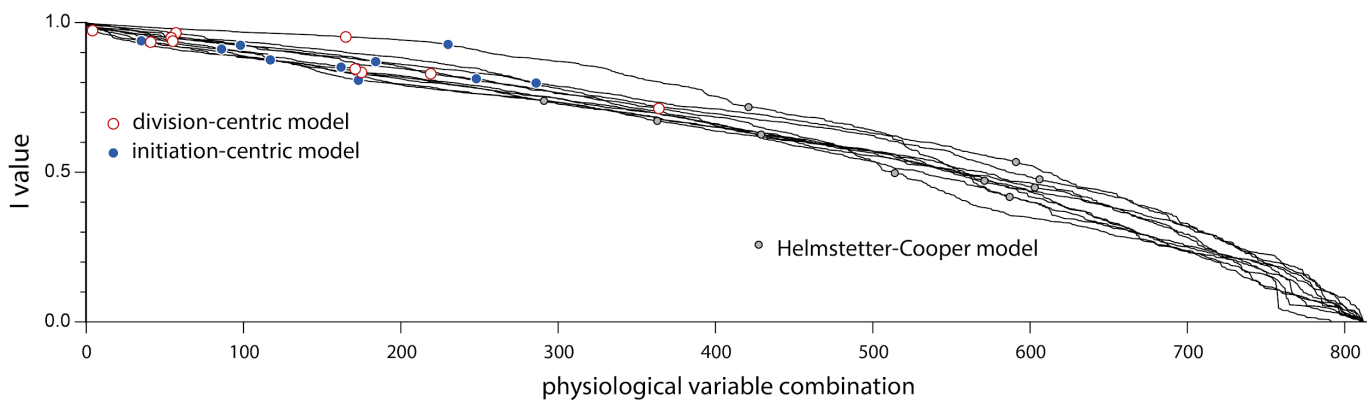


Figure 5: Ranked-order *I* values for combinations of 3 physiological variables for a total of 10 single-cell experiments: 4 experiments from Witz *et al.* (2019) and for 6 experiments from Si & Le Treut *et al.* (2019).

The replication-centric model by Witz *et al.* is incompatible with size homeostasis by adder.

In the presence of physiological fluctuations, the cell-size homeostasis mechanism ensures the return of cell-size to its steady-state value throughout several cell generations. A crucial quantity in cell size homeostasis is the mother/daughter (Pearson) correlation, ρ_d , for cell size at division. The adder principle is equivalent to having a correlation coefficient $\rho_d = 1/2$ as shown by many (Amir 2014; Taheri-Araghi *et al.* 2015; Voorn, Koppes, and Grover 1993; Material and Methods). However, the initiation-centric model by Witz *et al.* does not produce this result. Specifically, we obtained

$$\rho_d = \frac{1}{2} \left(1 + 3 \frac{\sigma_{id}^2}{\sigma_{ii}^2} \right)^{-1}, \quad \text{Eq. 1}$$

where σ_{id} and σ_{ii} are the standard deviations of δ_{id} and δ_{ii} , respectively (see Materials and Methods for derivation). Therefore, this correlation coefficient is always smaller than 1/2, and it only reproduces the “adder” behavior in the deterministic limit $\sigma_{id} \rightarrow 0$. The range of experimental values of σ_{id}/σ_{ii} is 0.5-1.3 in Witz *et al.*'s study and 0.6-2.7 in Si & Le Treut (2019). Therefore, the model by Witz *et al.* predicts significant deviations from the adder phenotype observed in experiments [data summarized in (Jun *et al.* 2018)], much closer to a sizer model ($\rho_d = 0$; Figure 6). We further confirmed these predictions using simulations (see the Simulation section in Materials and Methods).

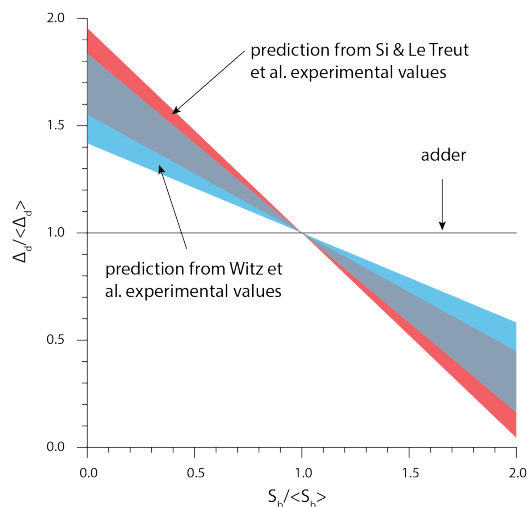


Figure 6: The theory based on the initiation-centric model predicts a more sizer-like behavior. We used Eq. 1 and the experimental values of σ_{id}/σ_{ii} from Witz *et al.* (2019) and Si & Le Treut *et al.* (2019).

Conclusion and outlook

Correlation analysis has become a powerful tool to interpret the flood of biological data enabled with the advent of high-throughput measurements. Correlations can indeed be a good starting point for a mechanistic model of the biological process under investigation. A case in point is the discovery of the original adder principle: the systematic lack of correlation between birth size and size added from birth to division in many conditions led to the formulation of a phenomenological model explaining how cell size converges toward a steady-state value.

However, correlation analysis can involve many variables, and the resulting complexity can be daunting and elude the original biological question. For example, in this work we showed that the model formulated on the basis of a correlation analysis does not in fact reproduce the adder principle. It is also a challenge to assess how sensitive on the experimental conditions the correlations are.

For this reason, a good strategy is to focus on correlations that are more robust than others across several conditions. Finding the control parameters that can change a seemingly invariant correlation should indeed give serious clues about the molecular mechanism that is responsible for it. Ideally, the control parameters should be linked to mechanistic hypotheses, such that they should change in response to biological perturbations that can be predicted and tested experimentally. We previously presented one such example to explain the mechanisms of cell-size control in bacteria (Si and Le Treut *et al.* 2019). We envision many other examples to emerge in connecting phenomenology and mechanisms in quantitative microbial physiology and beyond.

Materials and Methods.

Availability of analysis, results, and note

All the numerical results, including simulations, discussed in the main text are available with detailed notes in the GitHub repository: <https://github.com/junlabucsd/DoubleAdderArticle>.

Strains and growth conditions

The following strains were used in this study.

- BW25113: F- DE(araD-araB)567 lacZ4787(del)::rrnB-3 LAM- rph-1 DE(rhaD-rhaB)568 hsdR514. [Note that the genotype of BW27378 is F- DE(araD-araB)567 lacZ4787(del)::rrnB-3 LAM- rph-1 DE(rhaD-rhaB)568 hsdR514 DE(araH-araF)570(::FRT).]
- SJ_FS130: To construct this strain, we introduced Δ dnaN::<[dnaN-ypet] into BW25113 using P1 transduction.
- SJ_DL188: MG1655 F- λ - rph-1 dnaA msfGFP kan mCherry-dnaN

We used minimal MOPS media for the MG1655 experiments in Figure 3 and minimal M9 glucose media with and without uracil for the SJ_FS130 (BW25113 based) experiments in Figure 4.

Microfluidics, Microscopy and Image processing.

We used the same method as described in Si & Le Treut et al (2019).

I-value analysis.

Following the methodology proposed by Witz and colleagues, we first defined the covariance matrix $K = [k_{ij}]$ of the analyzed variables. Then the score was computed as:

$$I = \frac{\det(K)}{\prod_i k_{ii}}$$

where the k_{ii} are the diagonal elements of the covariance matrix, hence the variances.

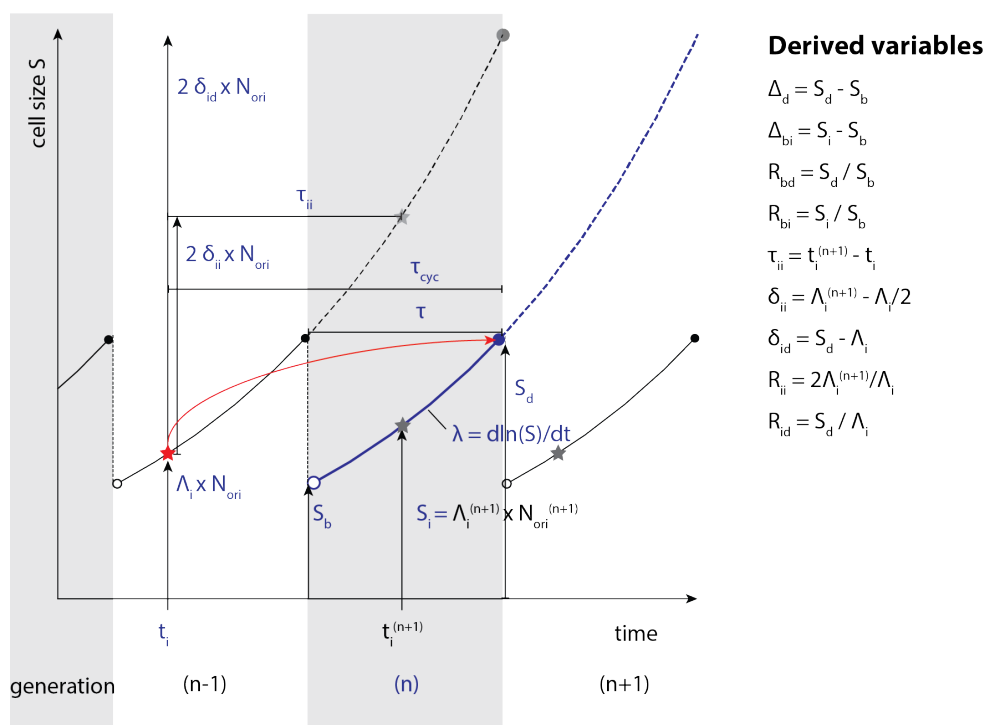


Figure S1: Definition of the physiological variables in a scenario with 2 overlapping cell cycles. All variables with blue font are associated with the current generation (n). We added a superscript when using physiological variables associated with another generation. We also defined variables derived from these quantities. Replication initiations are indicated with stars, and the red star is the initiation determining the division for the current generation. N_{ori} is the number of origins of replication just before initiation happens.

We defined 18 physiological variables in line with the definitions given by Witz *et al.* (see Figure S1): λ , S_b , S_d , S_i , Δ_d , Δ_{bi} , Λ_i , $\Lambda_i^{(n-1)}$, $\Lambda_i^{(n+1)}$, δ_{ii} , δ_{id} , R_{ii} , R_{id} , R_{bd} , R_{bi} , τ , τ_{cyc} and τ_{ii} . We generated all possible combinations of 3 variables, that is $C_{18}^3 = 816$. We emphasize the difference between Λ_i and S_i . The former is the cell size per origin of replication at the initiation event associated with the division in the current generation; therefore it could be in a previous generation (*e.g.* mother, grand-mother cell). The latter is the cell size when replication initiation occurs in the current generation. These 2 variables are only the same in the case of non-overlapping cell cycles.

We also found that the results of this analysis were sensitive to processing of the experimental data. In their work, Witz and colleagues, instead of using the measured values for S_b , S_d , S_i and Λ_i , first fitted traces of cell sizes to an exponential function and took values interpolated by this fit. Yet it did not affect the relative ranking of the division-centric model with respect to the initiation-centric model.

Parameters in the initiation-centric model by Witz *et al.* In their analysis, Witz *et al.* used 4 variables: Λ_i , δ_{ii} , δ_{id} and λ . However, Λ_i is not strictly required. Indeed, from the knowledge of Λ_i in the first cell of the lineage, one may reconstruct the subsequent replication and division cycles from the sole knowledge of δ_{ii} , δ_{id} and λ . Therefore Λ_i appears to be an initial condition, and the other 3 variables actually define a model for division and replication cycle progression.

Parameters in our division-centric model and in the Helmstetter-Cooper model. In our division-centric model, the cell size at birth S_b is only required in the first cell of the lineage. The knowledge of only the 3 variables δ_{ii} , Δ_d and λ in each new generation is sufficient to reconstruct the whole lineage. The Helmstetter-Cooper model

features the cell size at replication initiation per origin s_i , the duration of the cell cycle τ_{cyc} and the growth rate λ . Similarly to our model, the cell size at birth S_b is only required in the first cell of the lineage. Then, from this initial condition and the knowledge of the 3 variables s_i , τ_{cyc} and λ at each new generation, one can reconstruct the whole cell lineage.

In summary, only 3 variables are necessary and sufficient to self-consistently define the cell cycle and cell size. This is why we carried out this “determinant” analysis using each of the 3-variable sets that we just described. Nevertheless, we also examined inclusion of a fourth variable, and found that it did not affect our conclusions.

Theory: cell size homeostasis in Witz *et al.*'s initiation-centric model.

In the model proposed by Witz and colleagues, the cell size per origin at division is determined by the cell size at initiation per origin Λ_i , the added size per origin between consecutive replication initiation events δ_{ii} , and the added size per origin from replication initiation to cell division δ_{id} . The following relation holds:

$$S_d^{(n)} = \Lambda_i^{(n)} + 2 \delta_{id}^{(n)},$$

$$\Lambda_i^{(n+1)} = \frac{1}{2} \Lambda_i^{(n)} + \delta_{ii}^{(n)},$$

where the index as n denotes the generation (or division cycle). Under the assumption that $\delta_{ii}^{(n)}$ (resp. $\delta_{id}^{(n)}$) are independently and identically distributed Gaussian stochastic variables with mean μ_{ii} (resp. μ_{id}) and standard deviation σ_{ii} (resp. σ_{id}), it follows that $\Lambda_i^{(n)}$ and $S_d^{(n)}$ are also Gaussian stochastic variables. At large n , they converge to the limiting distributions $\Lambda_i \equiv N(\mu_i, \sigma_i)$ and $S_d \equiv N(\mu_d, \sigma_d)$, where:

$$\mu_i = 2 \mu_{ii}, \quad \sigma_i^2 = \frac{4}{3} \sigma_{ii}^2.$$

$$\mu_d = 2 (\mu_{ii} + \mu_{id}), \quad \sigma_d^2 = 4 \left(\frac{1}{3} \sigma_{ii}^2 + \sigma_{id}^2 \right).$$

The mother/daughter correlation for division size is a central quantity in cell size homeostasis, which can be derived in this model. As a first step, let us define the centered variables: $d\Lambda_i^{(n)} = \Lambda_i^{(n)} - \mu_i$ and $dS_d^{(n)} = S_d^{(n)} - \mu_d$. We then obtain the relations:

$$\langle d\Lambda_i^{(n+1)} \cdot d\Lambda_i^{(n)} \rangle = \frac{1}{2} \sigma_i^2,$$

$$\langle dS_d^{(n+1)} \cdot dS_d^{(n)} \rangle = \frac{1}{2} \langle d\Lambda_i^{(n+1)} \cdot d\Lambda_i^{(n)} \rangle,$$

where the brackets denote averages. We therefore obtain the mother/daughter Pearson correlation coefficients (in the large n limit):

$$\rho_i = \frac{\langle d\Lambda_i^{(n+1)} \cdot d\Lambda_i^{(n)} \rangle}{\sigma_i^2} = \frac{1}{2}.$$

$$\rho_d = \frac{\langle dS_d^{(n+1)} \cdot dS_d^{(n)} \rangle}{\sigma_d^2} = \frac{1}{2} \left(1 + 3 \frac{\sigma_{id}^2}{\sigma_{ii}^2} \right)^{-1}.$$

In this model the joint distribution $(S_d^{(n)}, S_d^{(n-1)})$ is a bivariate Gaussian, therefore we can write the conditional expectation of $S_d^{(n)}$ as:

$$\langle S_d^{(n)} | S_d^{(n-1)} \rangle = \rho_d S_d^{(n-1)} + (1 - \rho_d) \mu_d.$$

With the hypothesis of symmetrical division, namely $S_b^{(n)} = 2 S_d^{(n-1)}$, we obtain for the conditional expectation of the added size from birth to division:

$$\langle S_d - S_b \mid S_b \rangle = (2 \rho_d - 1) S_b + (1 - \rho_d) \mu_d.$$

Therefore, the “adder” principle is equivalent to having $\rho_d = 1/2$. From these results, the model proposed by Witz and colleagues always results in $2 \rho_d - 1 < 0$. In fact, it only reproduces the “adder” principle in the deterministic limit $\sigma_{id} \rightarrow 0$.

Simulations

In this study we have performed simulations of both initiation-centric and division-centric models. For this, we have re-used the code provided by Witz and colleagues (2019). Few and minor modifications have been made, but these modifications did not affect the outcome or the essence of the original simulations. Simulations performed consist of:

- Repeats of the simulations performed by Witz and colleagues in their original study.
- Simulations using Witz and colleagues original parameters, but with perfectly symmetrical division.
- Simulations of Witz et al. model, and our model, using experimental parameters taken from experimental datasets from Witz and et al. and datasets published in (Si and Le Treut et al. 2019).

See <https://github.com/junlabucsd/DoubleAdderArticle> for more details.

Deviations of Witz *et al.*'s initiation-centric model (simulation) from the adder behavior. Witz *et al.*'s simulation reproduced the adder behavior observed in their data, in apparent contradiction with our prediction in Eq. 1 that their initiation-centric model is inconsistent with size homeostasis by the adder. We analyzed their simulations and found that they produced the adder-like behavior because of the additional fluctuations in the septum position (Figure S2A).

Experimentally, septum position represents the most precise control among all measured single-cell parameters with $CV < 5\%$ (Taheri-Araghi et al. 2015; Sauls et al. 2019). Indeed, removing fluctuations in the septum position alone made the simulation deviated from experiment in a quantitative manner consistent with Eq. 1. We also conducted a similar analysis using our experimental data (Si and Le Treut et al. 2019), and reached the same conclusion (Figure S2B). Based on this observation, we conclude that the model proposed by Witz *et al.* does not self-consistently explain the adder phenotype.

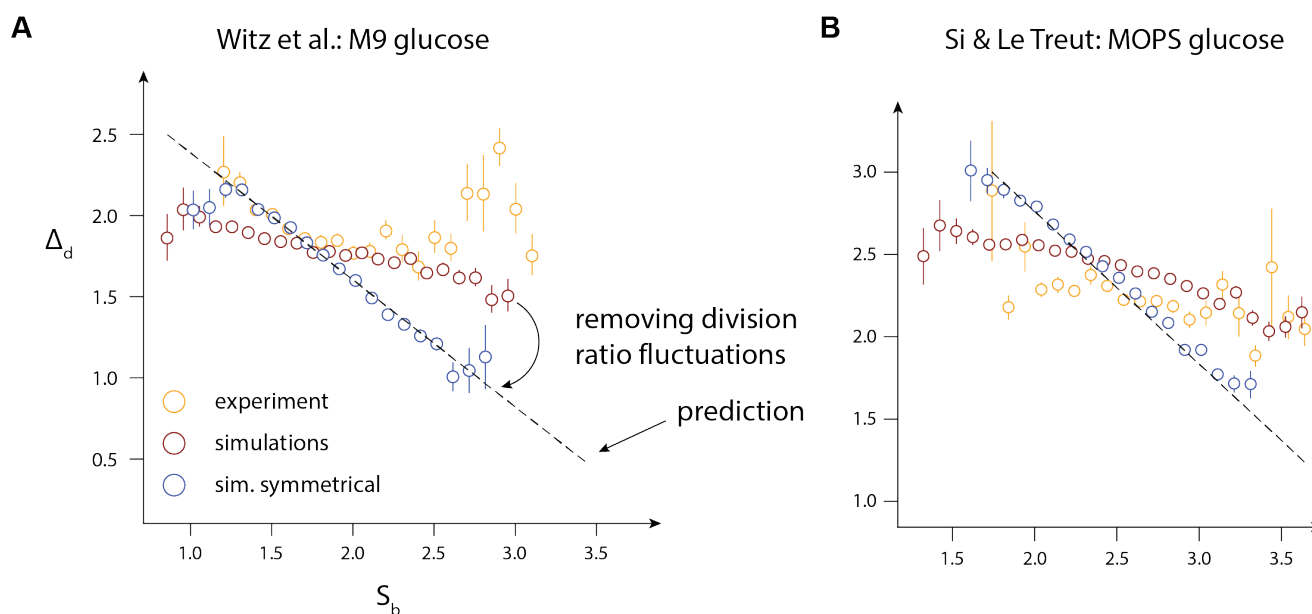


Figure S2: Agreement of the initiation-centric model with experimental data from **A.** Witz et al., M9 + glucose condition and **B.** Si & Le Treut et al., MOPS + glucose condition. **A.** The agreement of simulations with experimental data gets worse after removing fluctuations in the division ratio. **B.** The agreement of simulations with experimental data is not as good, and gets worse after removing fluctuations in the division ratio.

References

- Adicptaningrum, Aileen, Matteo Osella, M. Charl Moolman, Marco Cosentino Lagomarsino, and Sander J. Tans. 2015. "Stochasticity and Homeostasis in the E. Coli Replication and Division Cycle." *Scientific Reports* 5 (December): 18261.
- Amir, A. 2014. "Cell Size Regulation in Bacteria." *Physical Review Letters* 112: 208102.
- Amir, A. 2017. "Point of View: Is Cell Size a Spandrel?" *eLife* 6: e22186.
- Baba, Tomoya, Takeshi Ara, Miki Hasegawa, Yuki Takai, Yoshiko Okumura, Miki Baba, Kirill A. Datsenko, Masaru Tomita, Barry L. Wanner, and Hirotada Mori. 2006. "Construction of Escherichia Coli K-12 in-Frame, Single-Gene Knockout Mutants: The Keio Collection." *Molecular Systems Biology* 2 (1). <https://www.embopress.org/doi/abs/10.1038/msb4100050>.
- Campos, Manuel, Ivan V. Surovtsev, Setsu Kato, Ahmad Paintdakhi, Bruno Beltran, Sarah E. Ebmeier, and Christine Jacobs-Wagner. 2014. "A Constant Size Extension Drives Bacterial Cell Size Homeostasis." *Cell* 159 (6): 1433–46.
- Cooper, S., and C. E. Helmstetter. 1968. "Chromosome Replication and the Division Cycle of Escherichia coliBr." *Journal of Molecular Biology*. <https://www.sciencedirect.com/science/article/pii/0022283668904257>.
- Datsenko, K. A., and B. L. Wanner. 2000. "One-Step Inactivation of Chromosomal Genes in Escherichia Coli K-12 Using PCR Products." *Proceedings of the National Academy of Sciences of the United States of America* 97 (12): 6640–45.
- Jun, Suckjoon, Fangwei Si, Rami Pugatch, and Matthew Scott. 2018. "Fundamental Principles in Bacterial Physiology-History, Recent Progress, and the Future with Focus on Cell Size Control: A Review." *Reports on Progress in Physics* 81 (5): 056601.
- Jun, Suckjoon, and Sattar Taheri-Araghi. 2015. "Cell-Size Maintenance: Universal Strategy Revealed." *Trends in Microbiology* 23 (1): 4–6.

- Lesterlin, C., E. Gigant, F. Boccard, and O. Espéli. 2012. "Sister Chromatid Interactions in Bacteria Revealed by a Site-specific Recombination Assay." *The EMBO Journal*.
<https://www.embopress.org/doi/abs/10.1038/emboj.2012.194>.
- Männik, Jaana, Bryant E. Walker, and Jaan Männik. 2018. "Cell Cycle-Dependent Regulation of FtsZ in Escherichia Coli in Slow Growth Conditions." *Molecular Microbiology* 110 (6): 1030–44.
- Sauls, John T., Sarah E. Cox, Quynh Do, Victoria Castillo, Zulfar Ghulam-Jelani, and Suckjoon Jun. 2019. "Control of Bacillus Subtilis Replication Initiation during Physiological Transitions and Perturbations." *mBio* 10 (6). <https://doi.org/10.1128/mBio.02205-19>.
- Sekar, Karthik, Roberto Rusconi, John T. Sauls, Tobias Fuhrer, Elad Noor, Jen Nguyen, Vicente I. Fernandez, et al. 2018. "Synthesis and Degradation of FtsZ Quantitatively Predict the First Cell Division in Starved Bacteria." *Molecular Systems Biology* 14 (11): e8623.
- Si, Fangwei, Guillaume Le Treut, John T. Sauls, Stephen Vadia, Petra Anne Levin, and Suckjoon Jun. 2019. "Mechanistic Origin of Cell-Size Control and Homeostasis in Bacteria." *Current Biology: CB* 29 (11): 1760–70.e7.
- Si, Fangwei, Dongyang Li, Sarah E. Cox, John T. Sauls, Omid Azizi, Cindy Sou, Amy B. Schwartz, et al. 2017. "Invariance of Initiation Mass and Predictability of Cell Size in Escherichia Coli." *Current Biology: CB* 27 (9): 1278–87.
- Soupene, Eric, Wally C. van Heeswijk, Jacqueline Plumbridge, Valley Stewart, Daniel Bertenthal, Haidy Lee, Gyaneshwar Prasad, Oleg Paliy, Parinya Charernnoppakul, and Sydney Kustu. 2003. "Physiological Studies of Escherichia Coli Strain MG1655: Growth Defects and Apparent Cross-Regulation of Gene Expression." *Journal of Bacteriology* 185 (18): 5611–26.
- Sunako, Y., T. Onogi, and S. Hiraga. 2001. "Sister Chromosome Cohesion of Escherichia Coli." *Molecular Microbiology* 42 (5): 1233–41.
- Taheri-Araghi, Sattar, Serena Bradde, John T. Sauls, Norbert S. Hill, Petra Anne Levin, Johan Paulsson, Massimo Vergassola, and Suckjoon Jun. 2015. "Cell-Size Control and Homeostasis in Bacteria." *Current Biology: CB* 25 (3): 385–91.
- Voorn, W. J., L. J. H. Koppes, and N. B. Grover. 1993. "Mathematics of Cell Division in Escherichia Coli: Comparison between Sloppy-Size and Incremental-Size Kinetics." *Curr. Top. Mol. Gen* 1: 187–94.
- Wallden, Mats, David Fange, Ebba Gregorsson Lundius, Özden Baltekin, and Johan Elf. 2016. "The Synchronization of Replication and Division Cycles in Individual E. Coli Cells." *Cell* 166 (3): 729–39.
- Witz, Guillaume, Erik van Nimwegen, and Thomas Julou. 2019. "Initiation of Chromosome Replication Controls Both Division and Replication Cycles in E. Coli through a Double-Adder Mechanism." *eLife* 8 (November). <https://doi.org/10.7554/eLife.48063>.